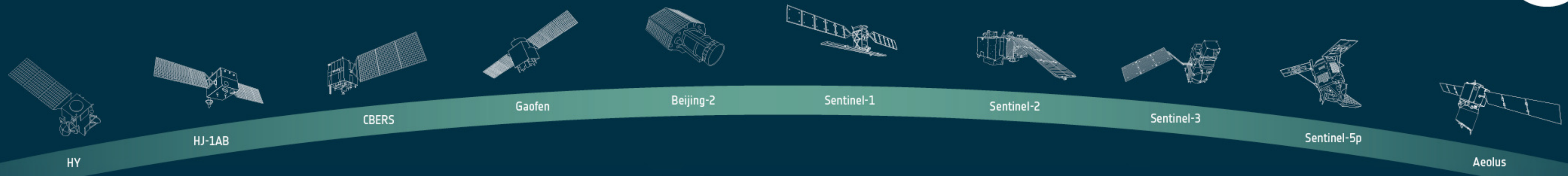

2022 DRAGON 5 SYMPOSIUM

MID-TERM RESULTS REPORTING

17-21 OCTOBER 2022

[PROJECT ID. 175]

FIRST LEVEL 1 PRODUCT RESULTS OF THE GREENHOUSE GAS MONITORING INSTRUMENT ON THE GAOFEN-5 SATELLITE

<18/OCT/2022, 10:20 AM-11:50 AM CEST>

ID. 175

PROJECT TITLE: FIRST LEVEL 1 PRODUCT RESULTS OF THE GREENHOUSE GAS MONITORING INSTRUMENT ON THE GAOFEN-5 SATELLITE

PRINCIPAL INVESTIGATORS: HAILING SHI, JOCHEN LANDGRAF

CO-AUTHORS: ZHIWEI LI, HANHAN YE, HAIYAN LUO, WEI XIONG

PRESENTED BY: HAILING SHI

- Objective
- Overview of the GMI
- Level 1 Processing Algorithm
- Geometric Correction Algorithms
- Level 1 Product Results
- Retrieval Results
- Plans

Objective

- THE GF-5(GAOFEN-5) satellite is the latest satellite to achieve hyperspectral resolution observations in the CHEOS (China High-Resolution Earth Observation System.)
- It was successfully launched from the Taiyuan Satellite Launch Center in May 2018
- GMI is mainly used to obtain global column concentration data on the GHGs carbon dioxide (CO2) and methane (CH4)

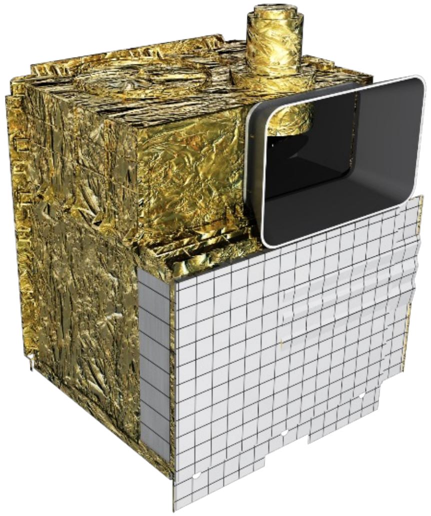

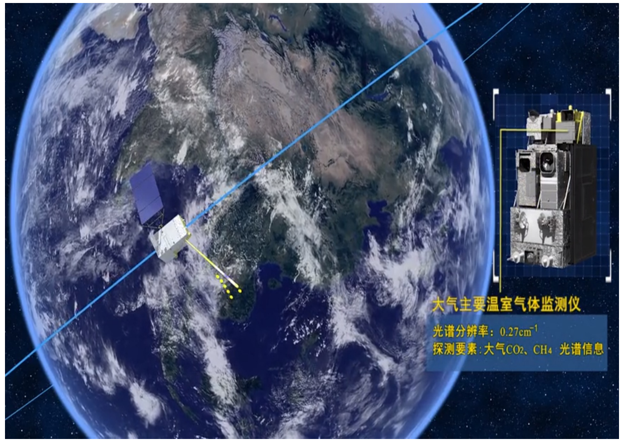

Objective

- the GMI payload on the GF-5 satellite adopts a novel form of spectroscopy, namely, SHS, to obtain the atmospheric absorption spectrum.

- The mechanism of the GMI is different from TANSO-Fourier transform spectroscopy (FTS)/GOSAT (Michelson interferometer) and OCO-2 (Grating), the data processing algorithms are quite different.

- The main objective is to introduce the processing algorithm for the Level 1 product (radiance spectrum) developed for the GMI and to discuss the first results of the hyperspectral-resolution spectrum from the GMI.

Overview of the GMI

Instrument

- the GMI payload on the GF-5 satellite adopts a novel form of spectroscopy, namely, SHS, to obtain the atmospheric absorption spectrum.
- Compared with a conventional Michelson interferometer, the SHS interferometer replaces the moving mirrors with diffraction gratings, resulting in extremely high spectral resolution within a narrow band.

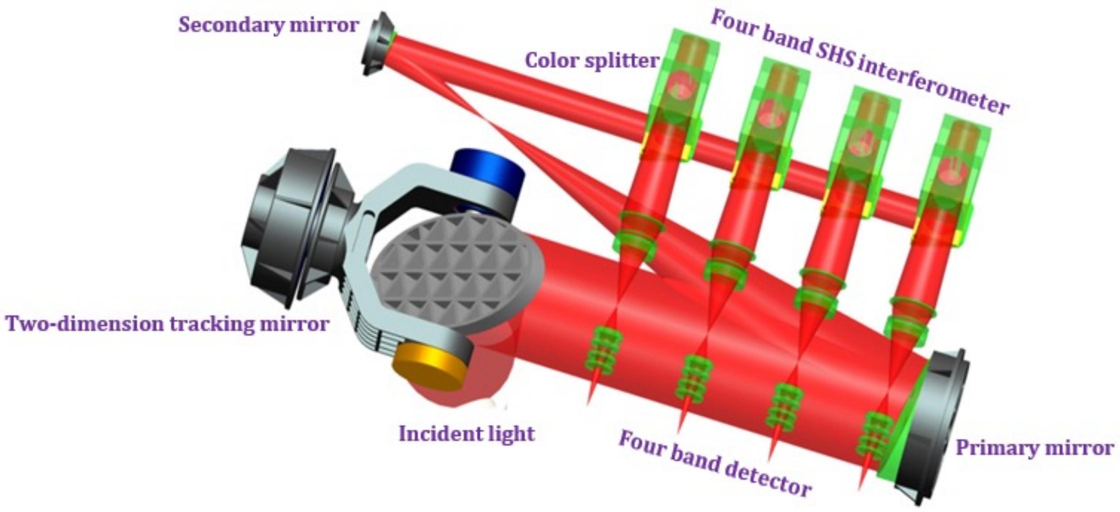

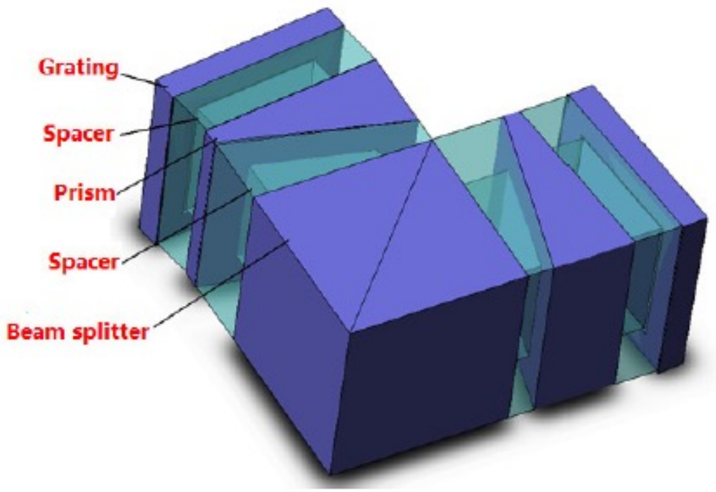

Overview of the GMI

Instrument

Specifications of the GMI

Specifications	Values			
	Band 1	Band 2	Band 3	Band 4
Detected gas	O_2	CO_2	CH_4	CO_2
Band range (μm)	0.759-0.769	1.568-1.583	1.642-1.658	2.043-2.058
Spectral resolution (cm^{-1})	0.6	0.27		
SNR (albedo=0.3; sun elevation=30°)	300		250	
Radiometric calibration	absolute accuracy: 5%, relative accuracy: 2%			
FOV	14.6 mrad (10.3 km @ 705 km)			
Scan	Cross track (, Along track ( )			
Observation modes	Nadir: 1, 5, 7, 9 points (default mode is 5 points); Sun glint; Calibration			
Number of detector pixels	1024×1024	512×640	512×640	256×320

Overview of the GMI

Instrument

To improve the data accuracy, the GMI is going to carry out a calibration, the 2-D tracking mirror is adjusted from the nadir/sun-glint observation mode to the calibration mode

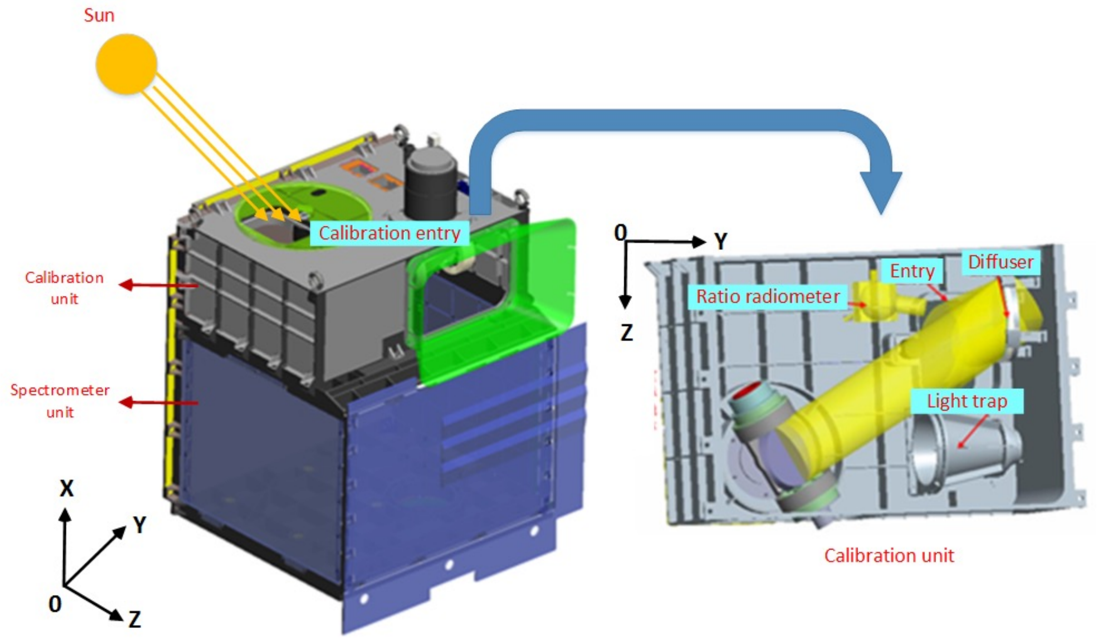

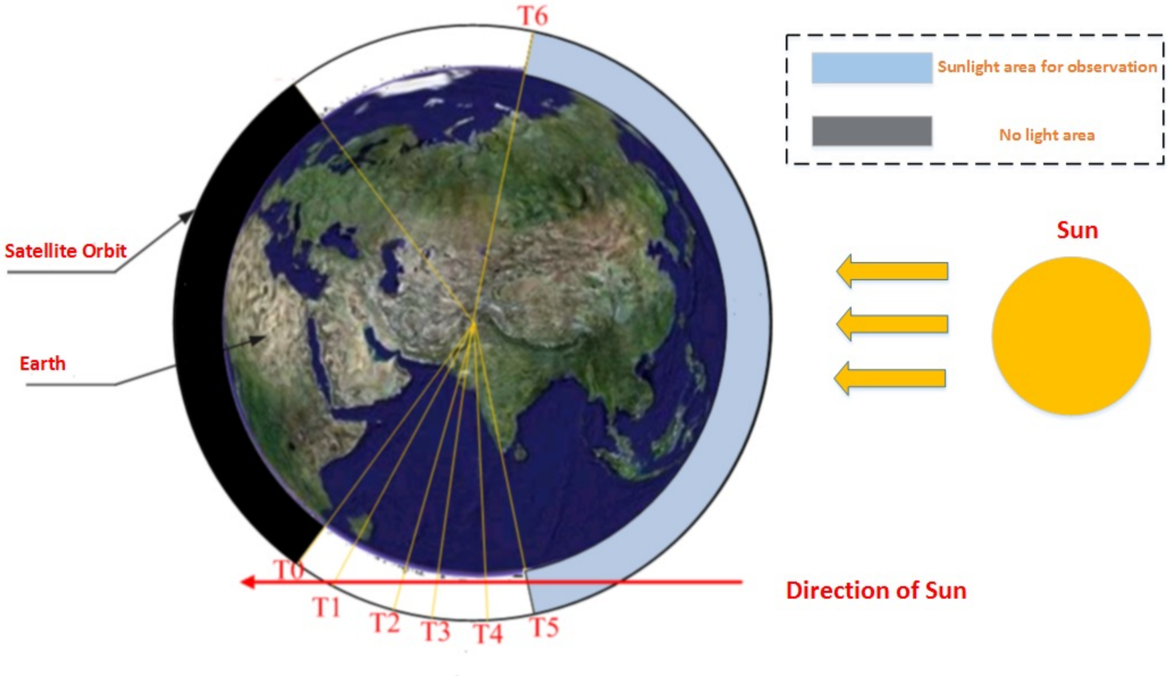

Overview of the GMI

Products

- Level 0: The original data obtained by the GMI are in the form of an interferogram
- Level 1: The radiance spectrum obtained through the processing of error correction, Fourier transform, spectral calibration, and radiation calibration of the satellite downloaded detection data
- Level 2: global column concentration distribution data of CO_2 and CH_4
- Level 3: the global carbon flux and 3-D distribution of CO_2 and CH_4

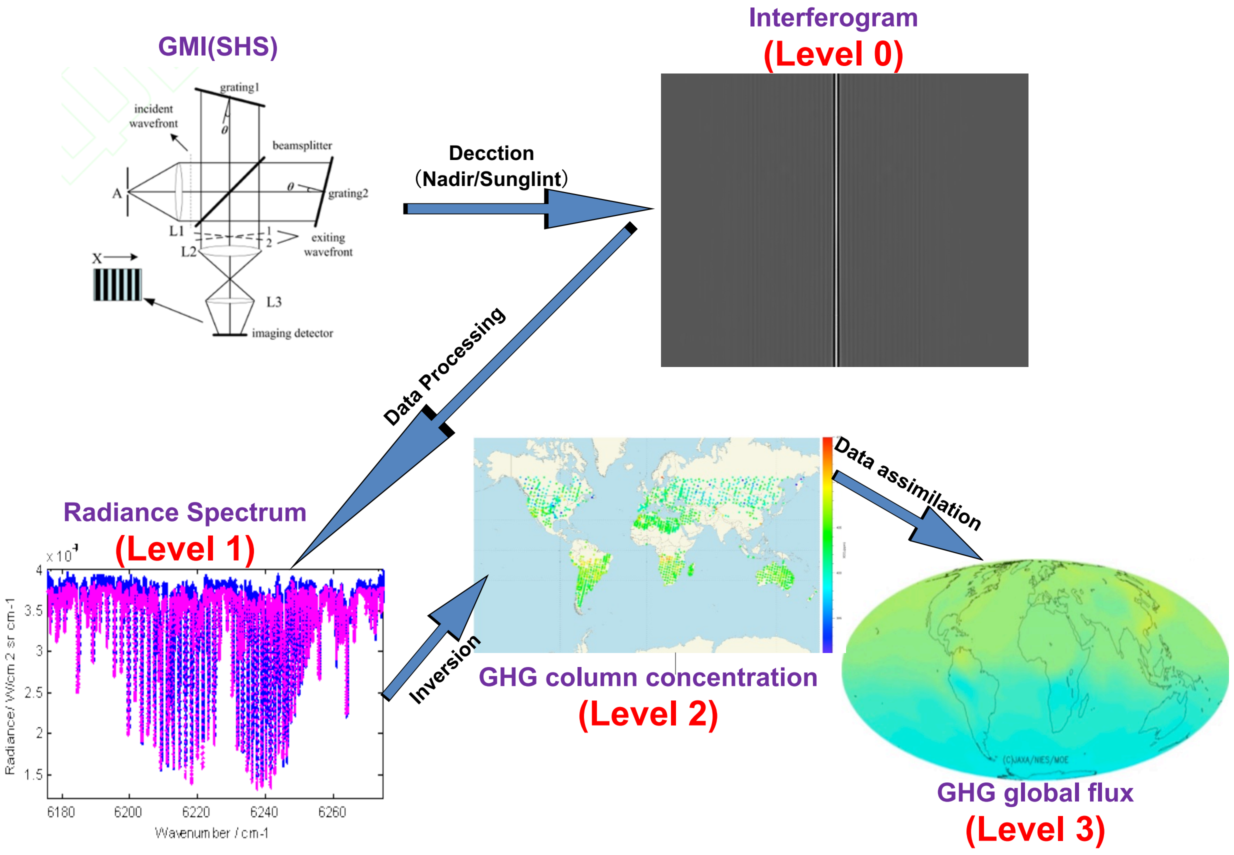

Level 1 Processing Algorithm

Interferogram
(Level 0)

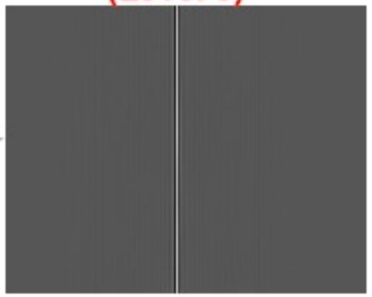

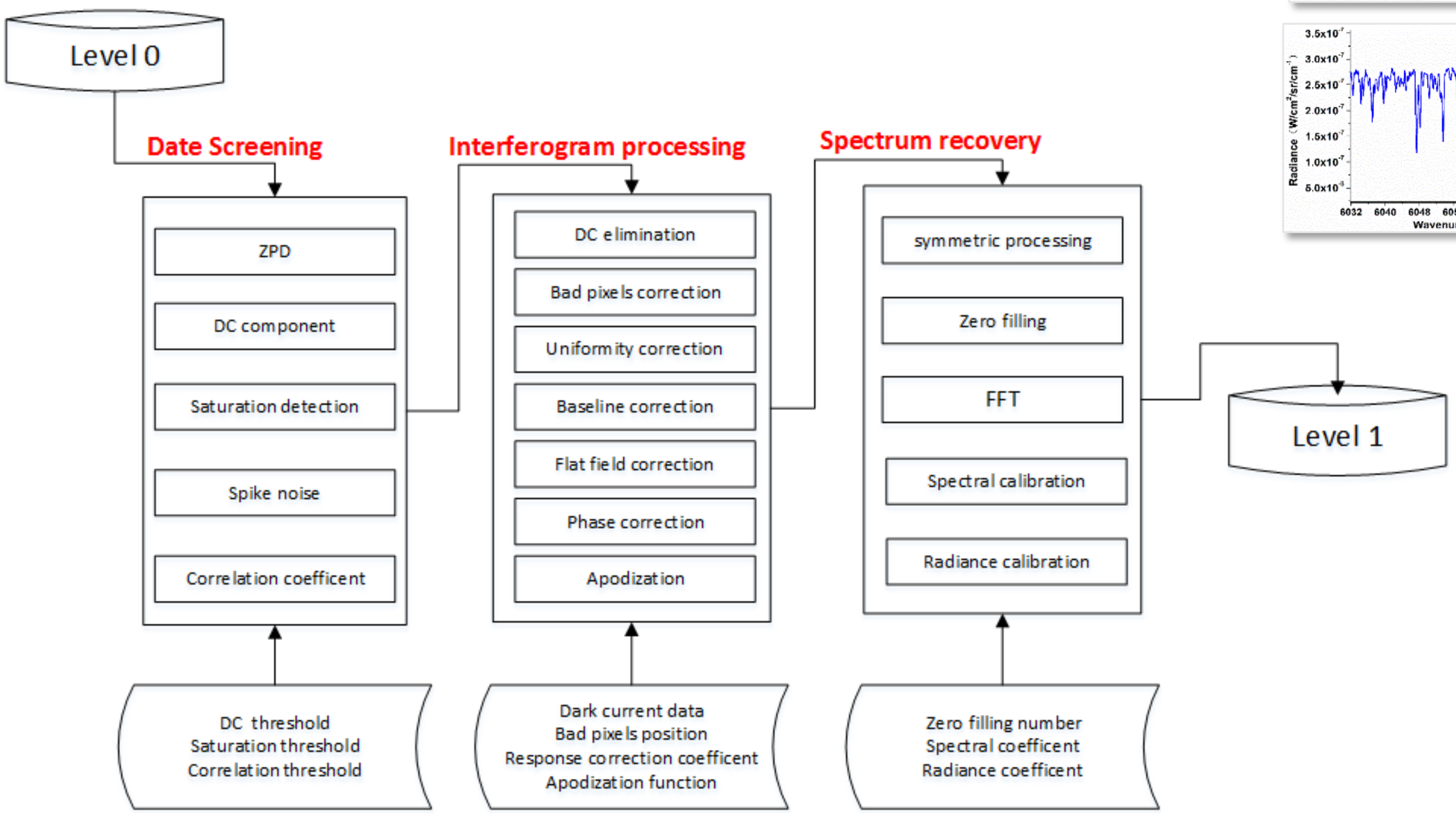

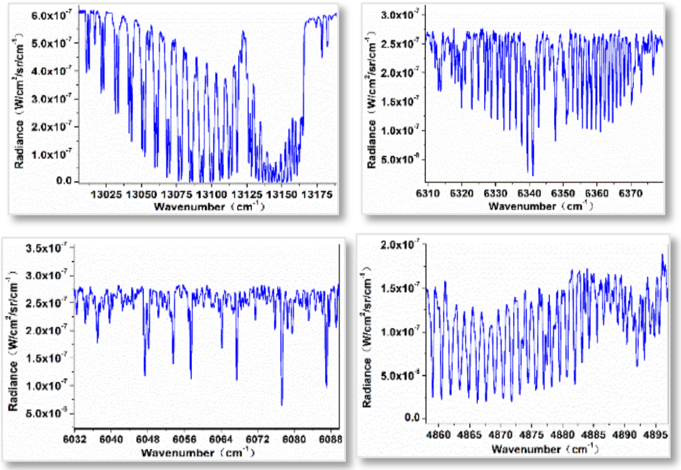

Radiance Spectrum
(Level 1)

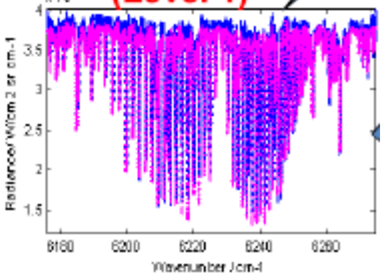

Level 1 Processing Algorithm

Data Screening

ZPD Deviation	ZPD position different from the normal value
Low SNR	Low SNR which is sampled above surface with low reflectivity
Saturation Detection	Saturated by an area with high reflectivity or cloud coverage
Spike Noise	With spike noise influenced by the space environment
Correlation Coefficients	Without effective modulation information

Level 1 Processing Algorithm

Interferogram Processing

- *Bad Pixel Correction*
- *Baseline Elimination*
- *Flat-Field Correction*
- *Phase Correction*
- *Apodization*

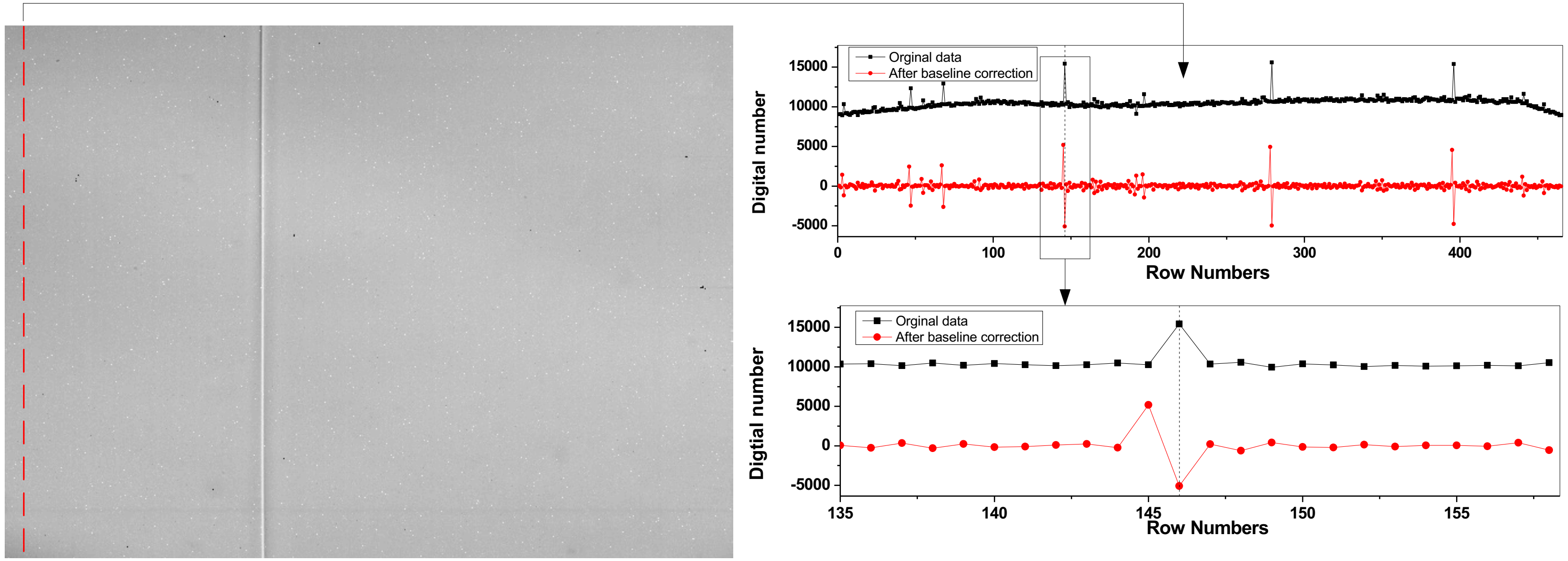

Interferogram Processing

Bad Pixel Correction

↓

Baseline Elimination

↓

Flat-Field Correction

↓

Phase Correction

↓

Apodization

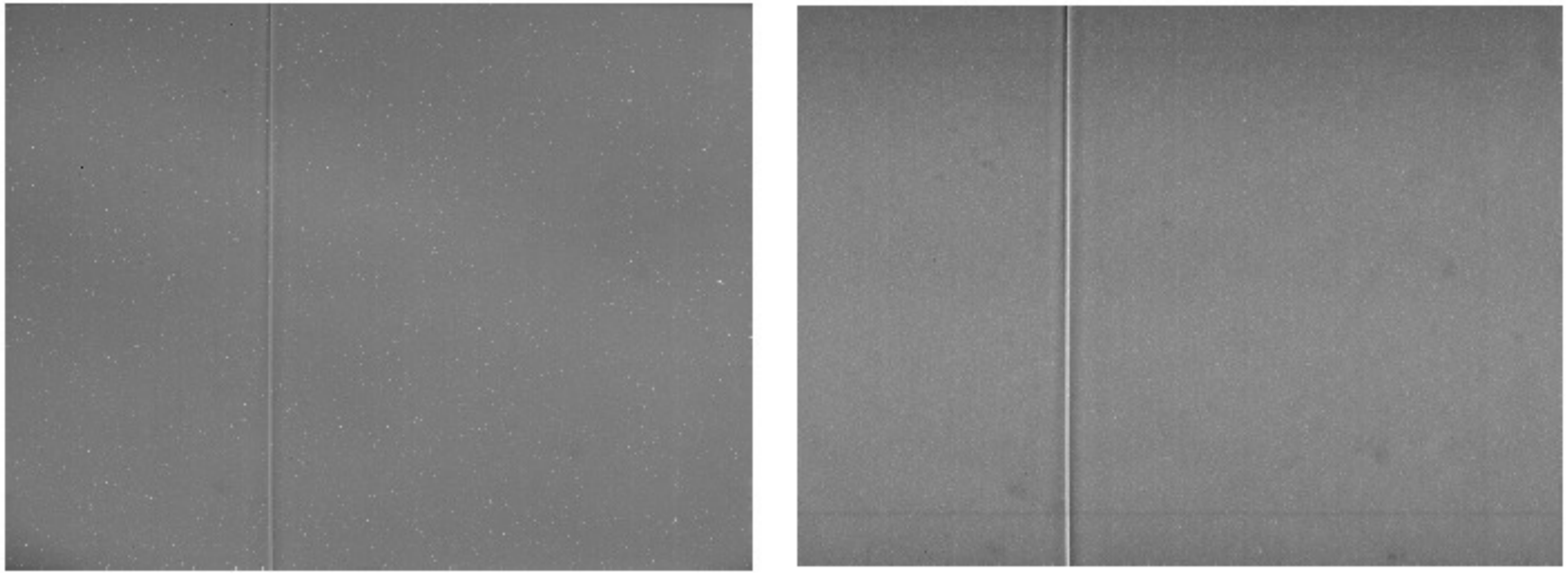

Bad pixel correction result (GMI Band 2 interferogram). (Left) Before correction. (Right) After correction.

Level 1 Processing Algorithm

Interferogram Processing

- *Bad Pixel Correction*
- *Baseline Elimination*
- *Flat-Field Correction*
- *Phase Correction*
- *Apodization*

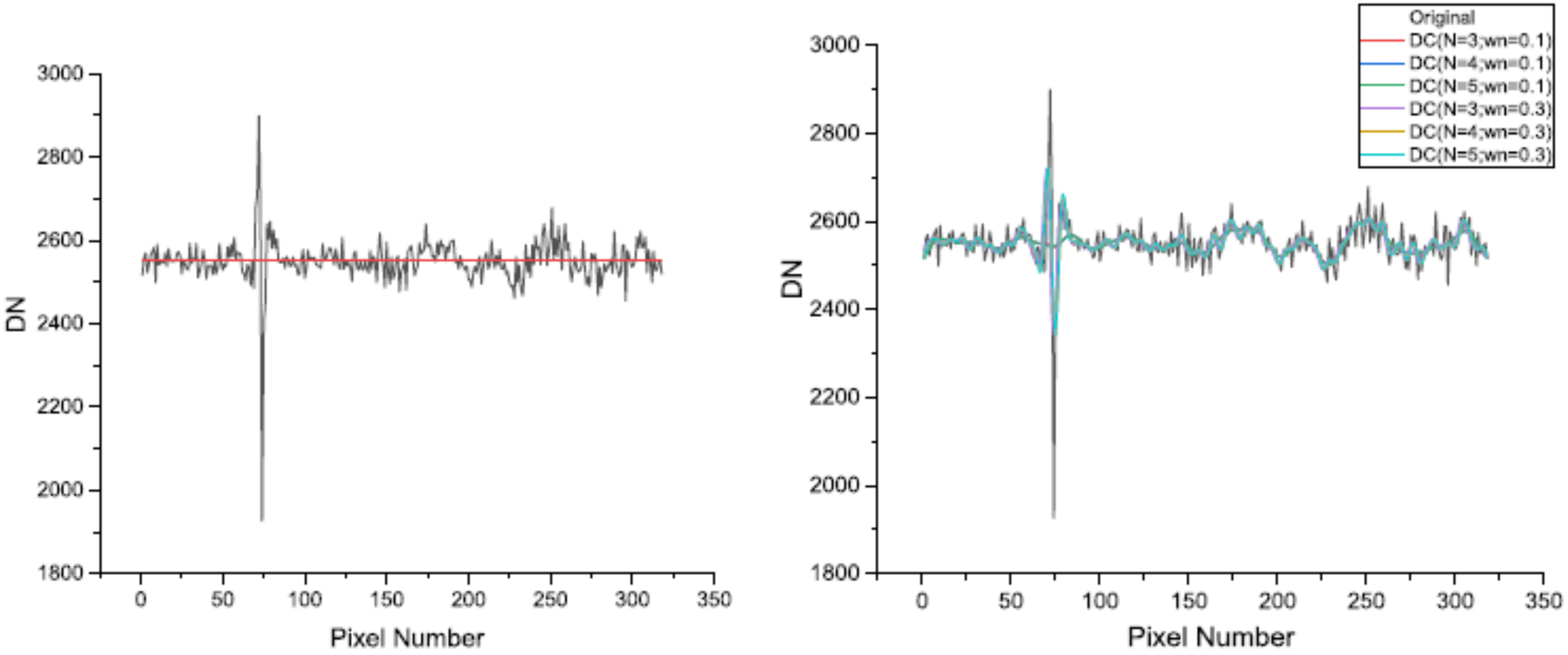

Baseline elimination results (GMI Band 3 interference fringe). (Left) Polynomial fitting method. (Right) Butterworth low-pass filter method.

Level 1 Processing Algorithm

Interferogram Processing

- *Bad Pixel Correction*
- *Baseline Elimination*
- *Flat-Field Correction*
- *Phase Correction*
- *Apodization*

- The SHS interferometer adopts the area array detector to collect the interference fringes simultaneously. This method has better stability, but at the same time, it also introduces a nonuniform response factor that the Michelson interferometer does not have
- The traditional flat-field method is not applicable, To solve the problem of SHS flat-field correction, the balanced arm flat-field method has been used

Level 1 Processing Algorithm

Interferogram Processing

Bad Pixel Correction

↓

Baseline Elimination

↓

Flat-Field Correction

↓

Phase Correction

↓

Apodization

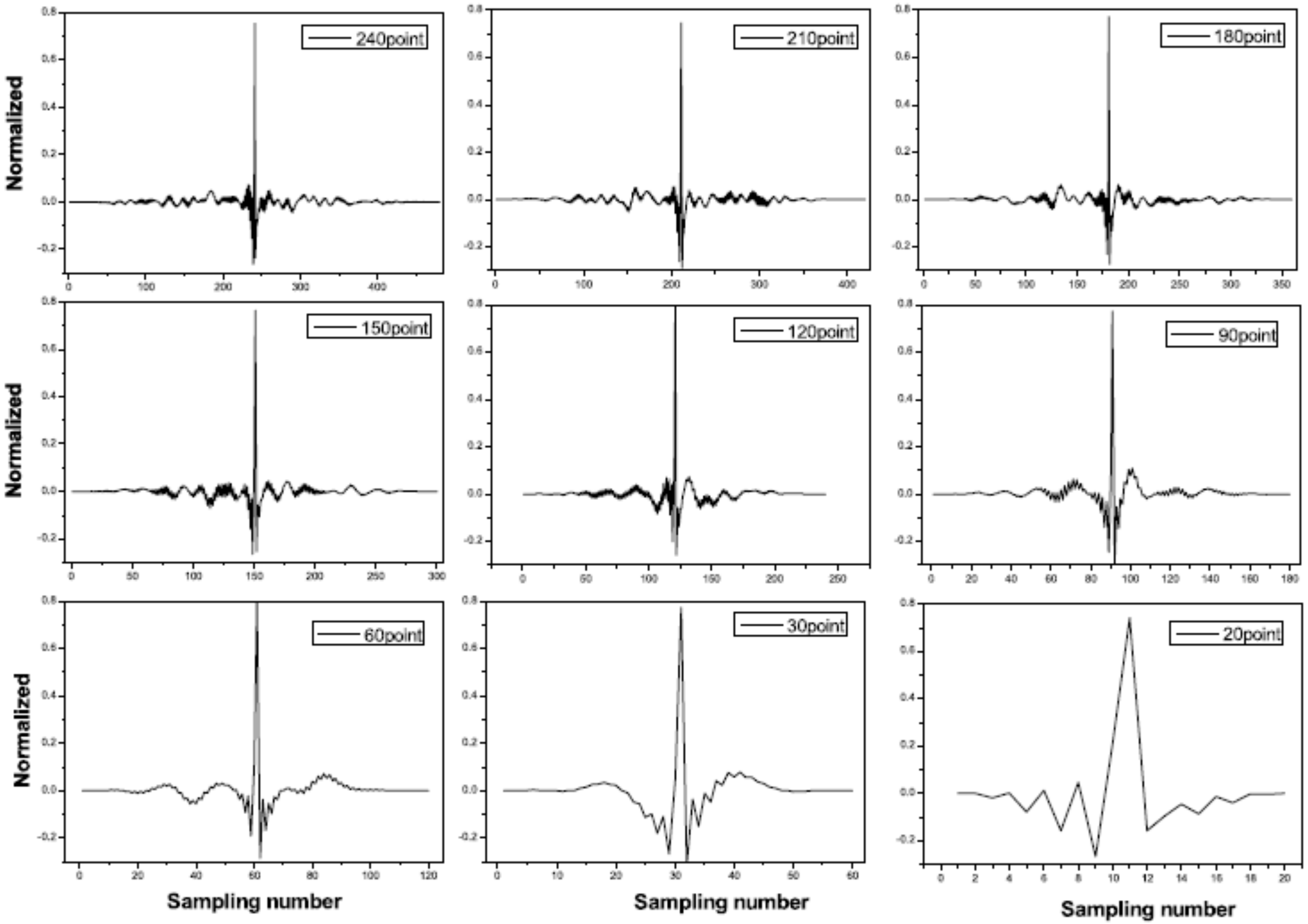

Level 1 Processing Algorithm

Interferogram Processing

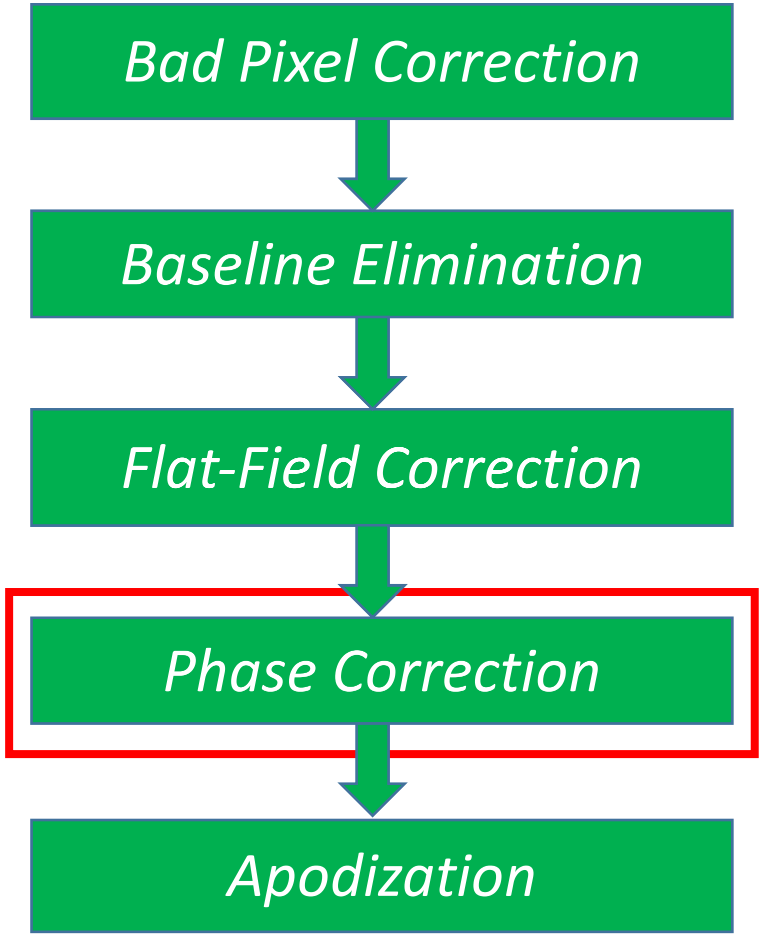

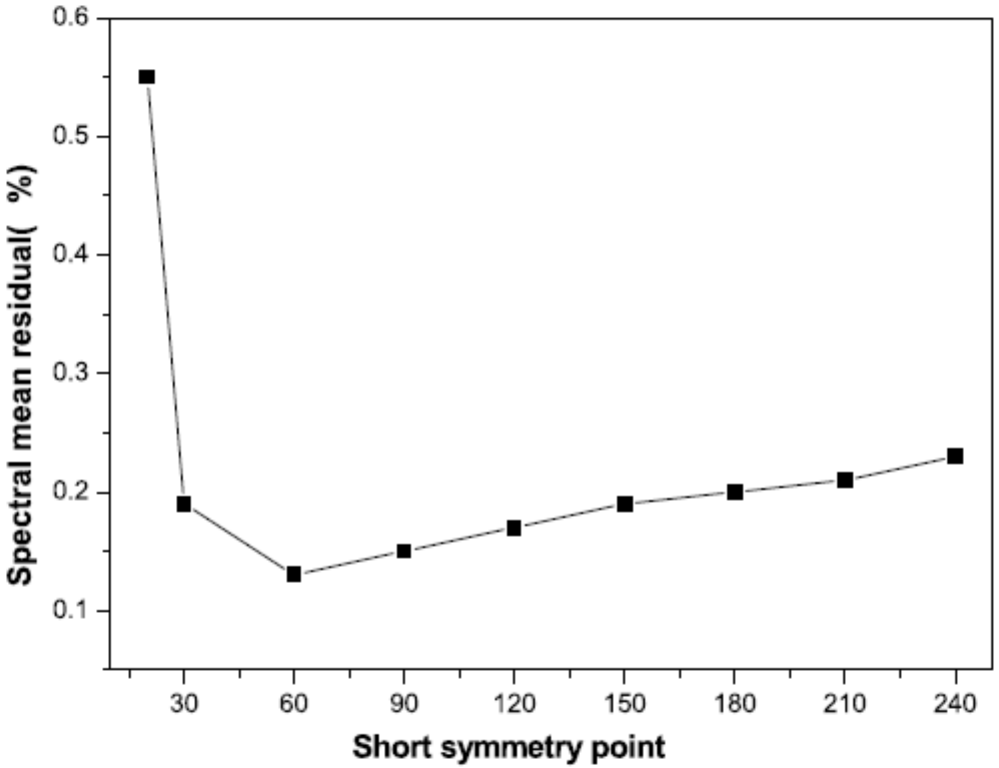

Level 1 Processing Algorithm

Interferogram Processing

- *Bad Pixel Correction*
- *Baseline Elimination*
- *Flat-Field Correction*
- *Phase Correction*
- ***Apodization***

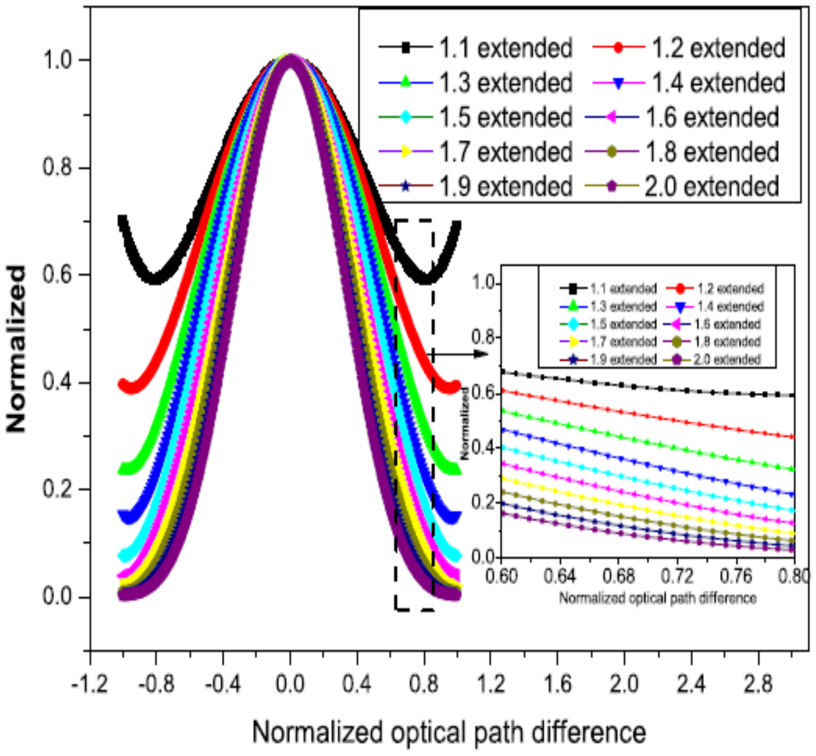

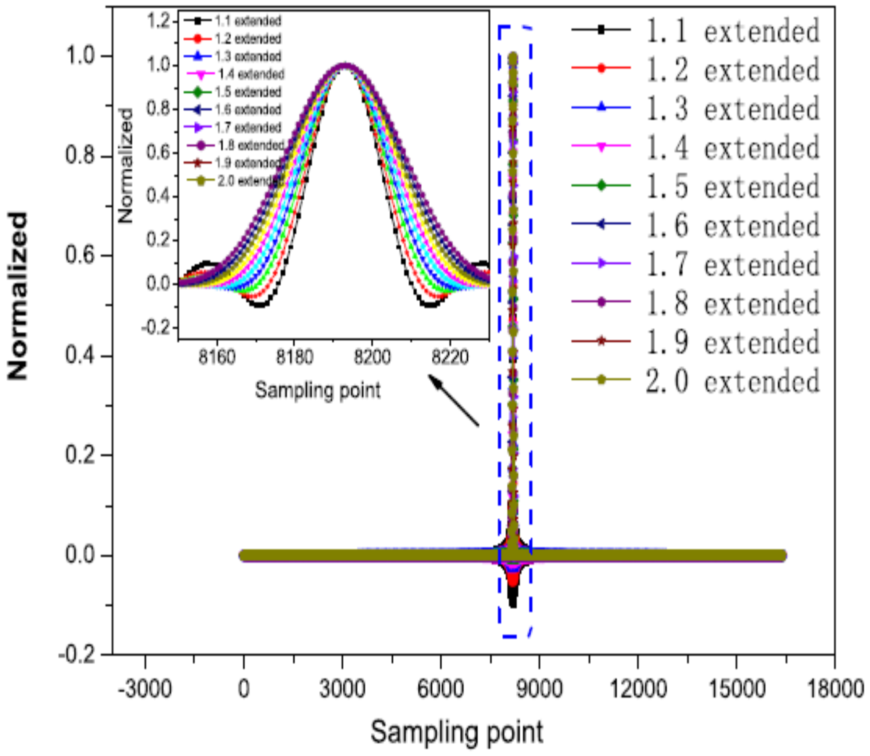

Level 1 Processing Algorithm

Spectrum Recovery

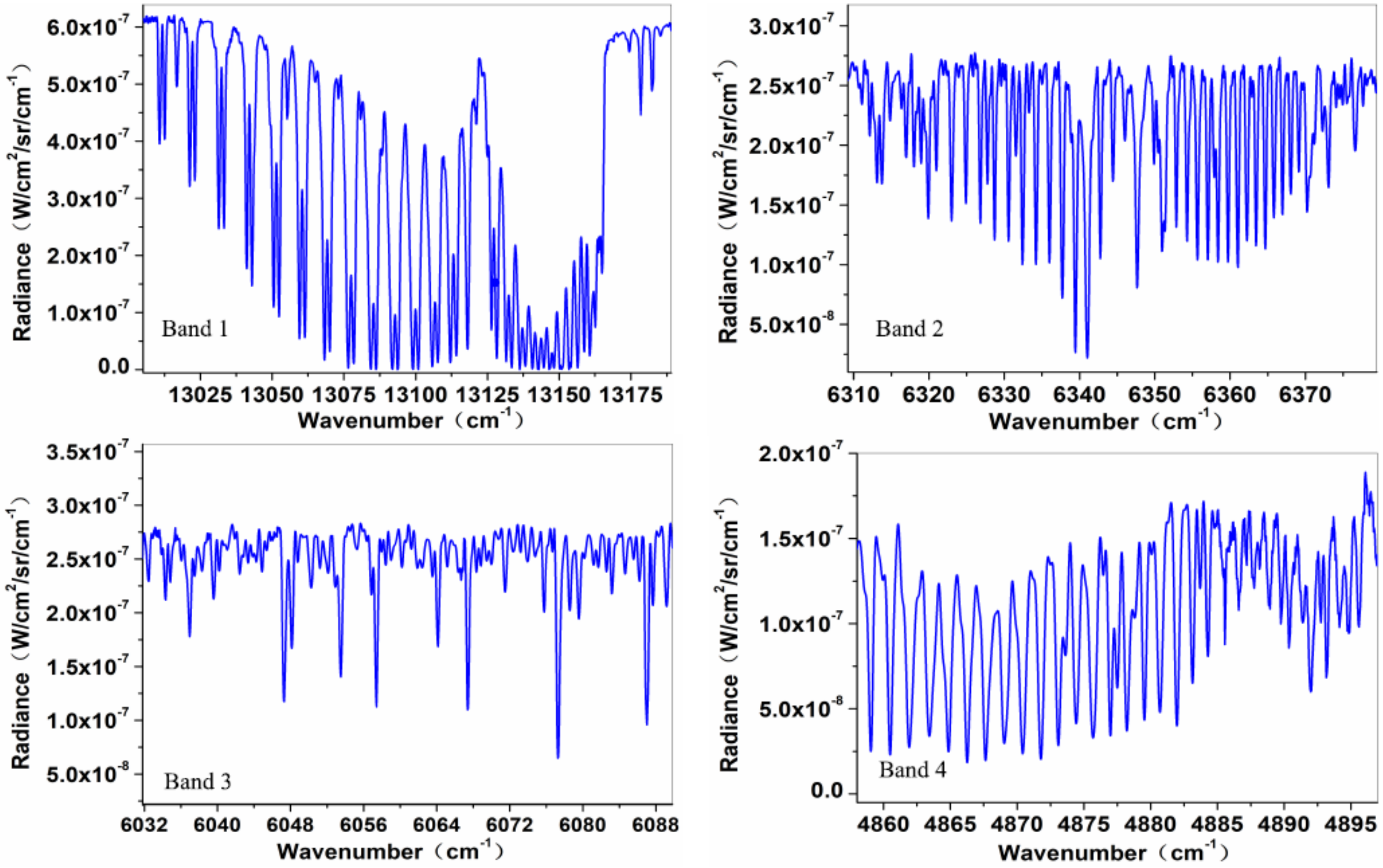

Geometric correction algorithms

Method

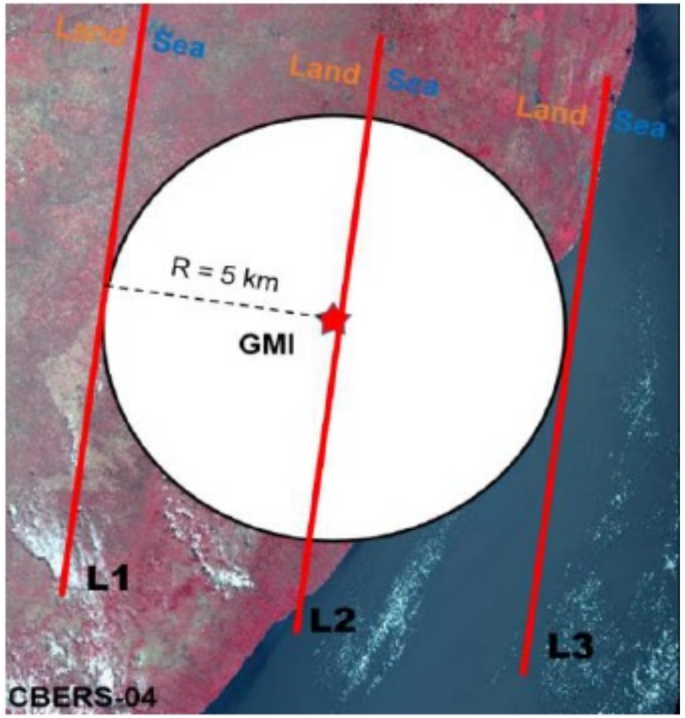

- L1: the observation point is tangent to the coastline and is located on the land, which reflectivity is high
- L2 (the observation point is tangent to the coastline)
- L3: the observation point is tangent to the coastline and is located in the ocean, which reflectivity is weak

$$I_c = a \cdot I_L + b \cdot I_S$$
$$a + b = 1.$$

$$I_{j-1} \leq I_j \leq I_{j+1}, \quad I_j \in [T_1, T_2]$$

or

$$I_{j-1} \geq I_j \geq I_{j+1}, \quad I_j \in [T_1, T_2]$$

Geometric correction algorithms

Results

$$
\begin{aligned}
\text{lon}' &= 1.00154 \cdot \text{lon} + 0.00119 \\
\text{lat}' &= 0.98858 \cdot \text{lat} + 0.01147.
\end{aligned}
$$

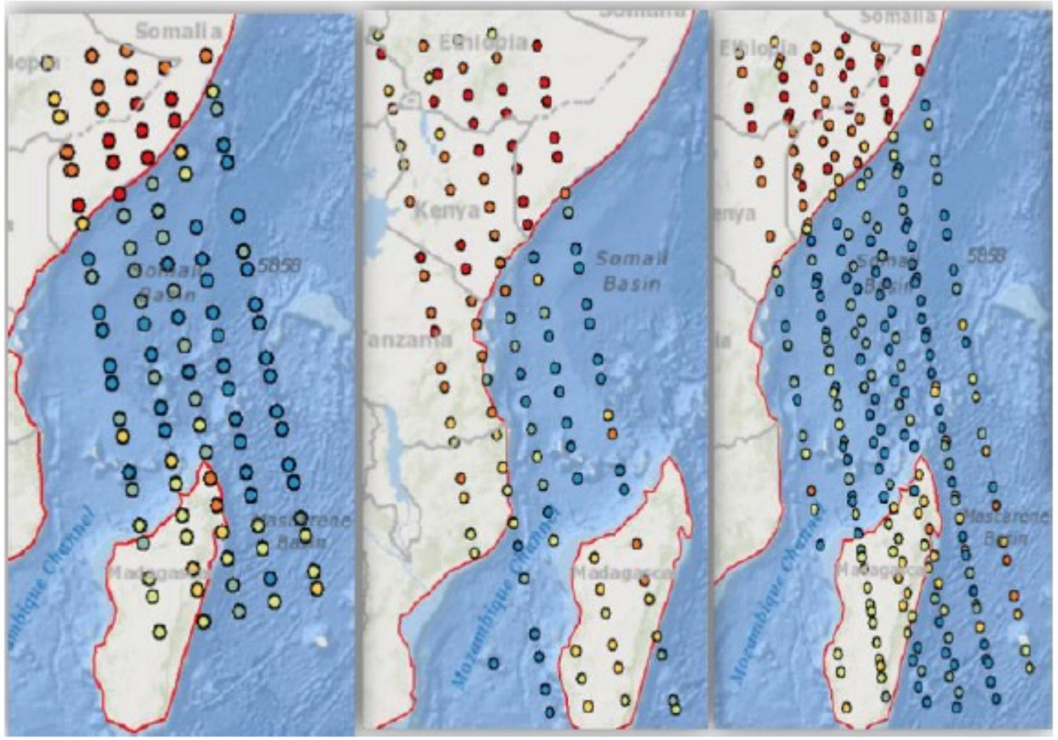

Point	GMI		WFI		Error	
	lon	*lat*	*lon*	*lat*	δlon	δlat
1	-20.710	48.610	-20.709	48.481	-0.001	0.129
2	-0.707	42.315	-0.663	42.277	-0.044	0.038
3	0.611	43.777	0.664	43.595	-0.053	0.182
4	-3.126	40.362	-3.105	40.131	-0.021	0.231
5	-20.749	48.419	-20.735	48.471	-0.014	-0.052
6	-13.723	40.546	-13.716	40.588	-0.007	-0.042
7	-0.205	42.681	-0.207	42.685	0.002	-0.004
8	0.560	43.643	0.657	43.581	-0.097	0.062
9	-2.765	40.145	-2.778	40.224	0.013	-0.079
10	-5.714	38.873	-5.677	38.820	-0.037	0.053
11	-7.262	39.195	-7.218	39.404	-0.044	-0.209
12	-9.934	39.751	-9.874	39.861	-0.060	-0.110

Level 1 Product Results

Satellite

- sun-synchronous orbit at an altitude of 705 km with an equatorial crossing local time descending node (LTDN) of 13:30
- completes an orbit in approximately 100 min and operates on a global basis with a 7-day orbit repeat cycle but with a 51-day footprint revisit cycle
- 1–9 cross-track points within +/−35◦of nadir, yielding an ~750-km cross-track range

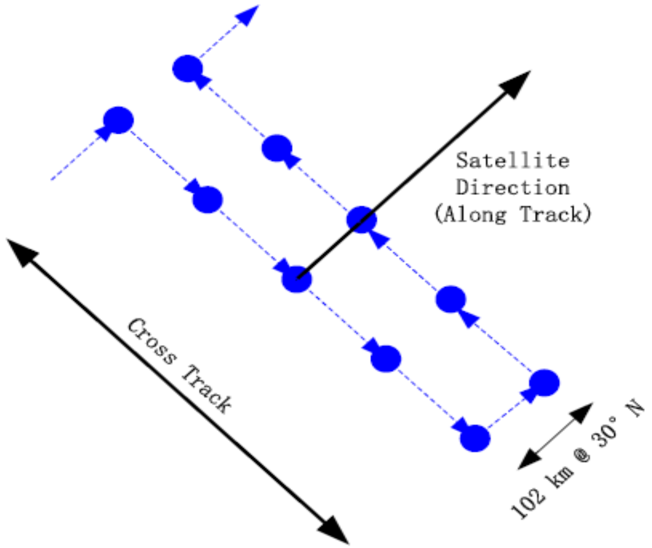

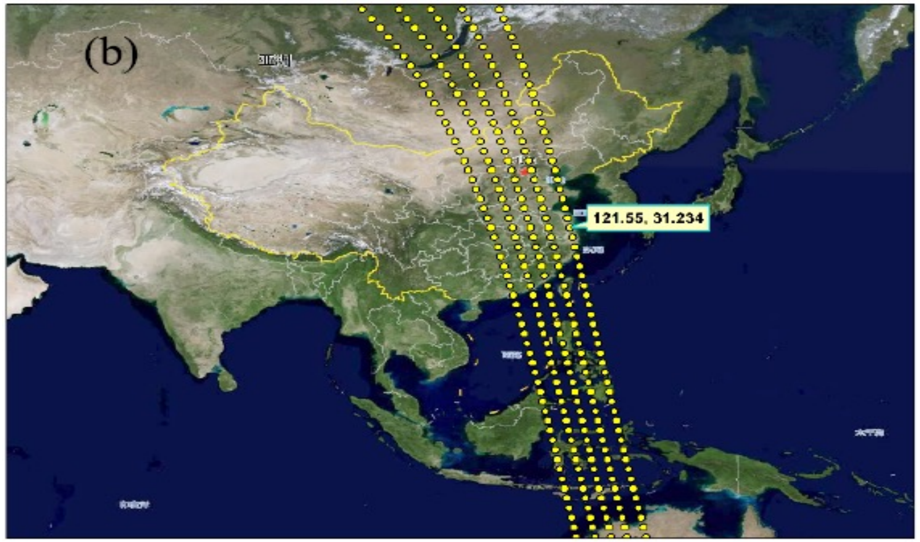

GMI grid point observations in the five-point cross-track scan mode

Level 1 Product Results

Spectral Resolution

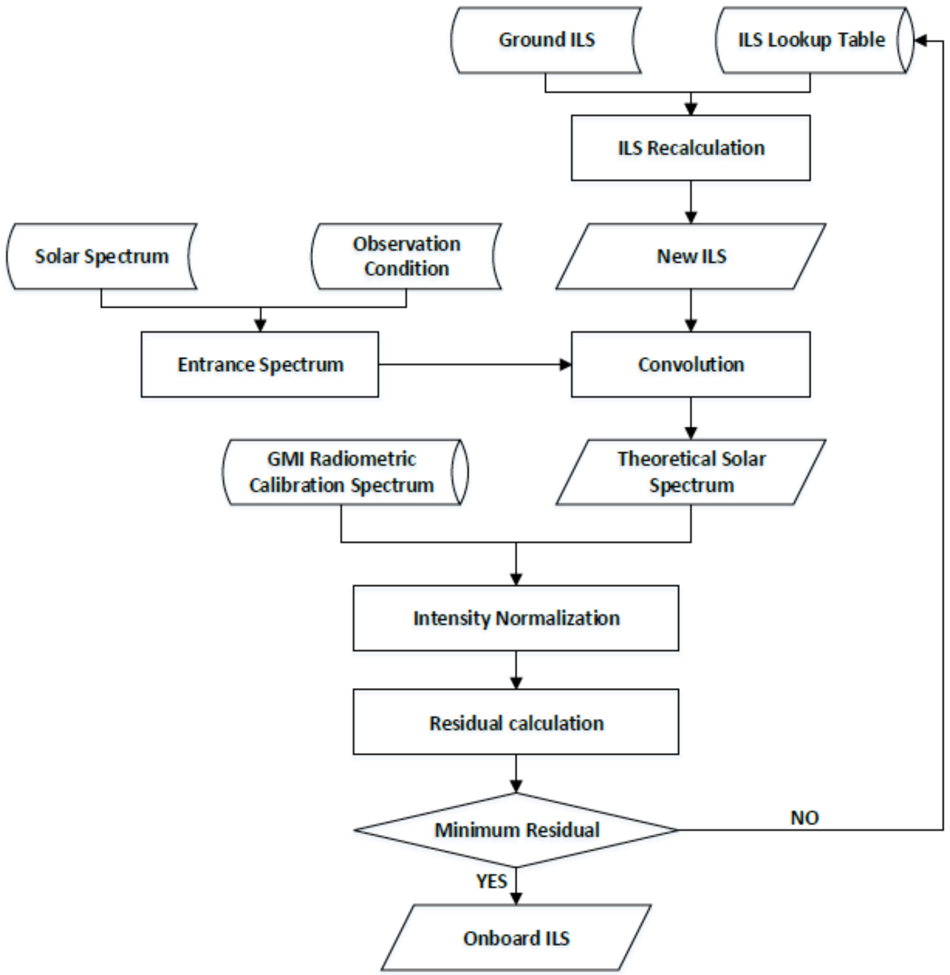

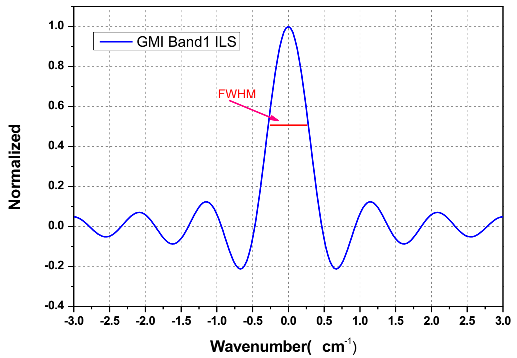

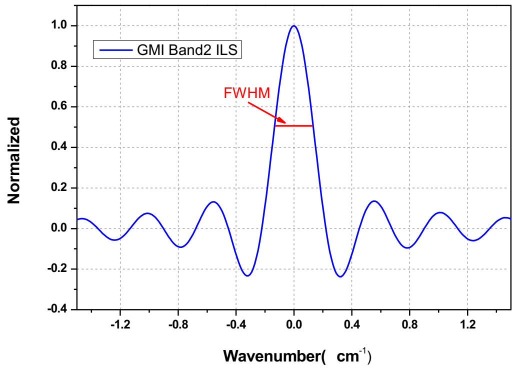

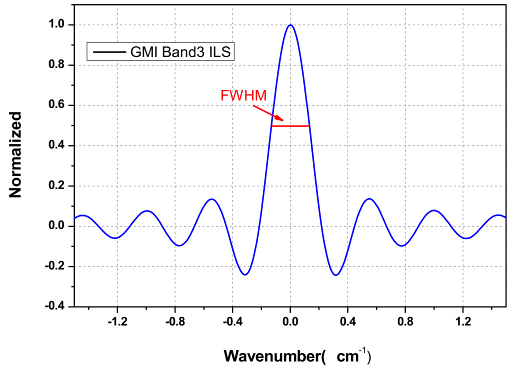

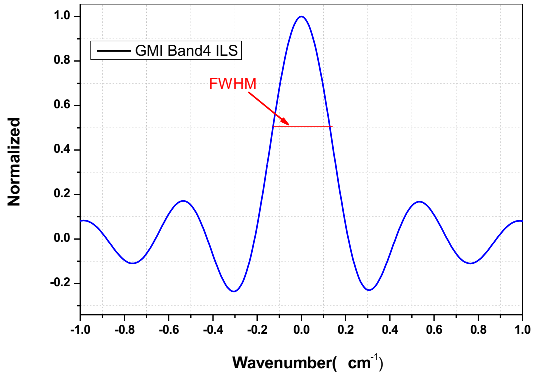

Level 1 Product Results

SNR

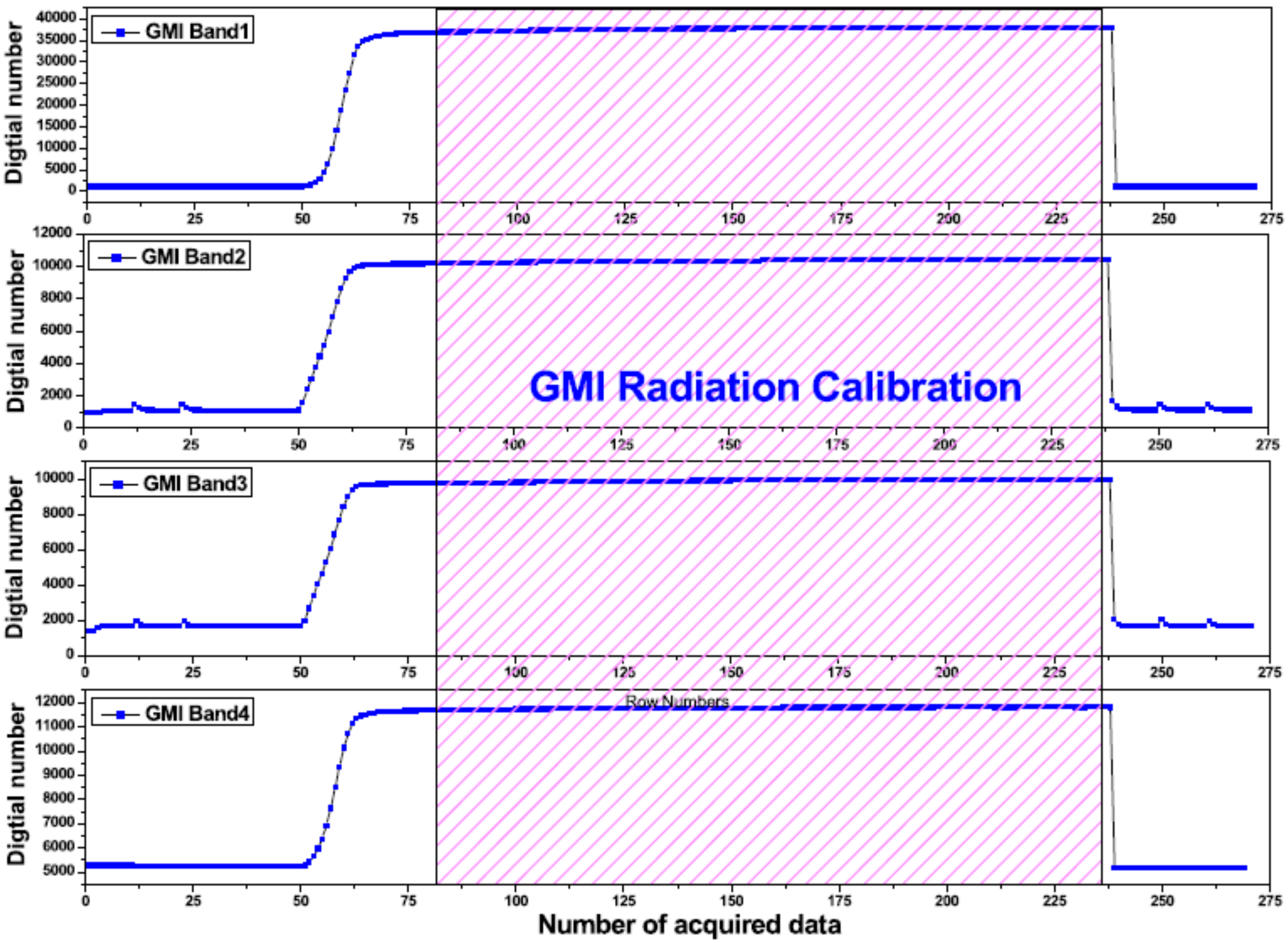

Level 1 Product Results

SNR

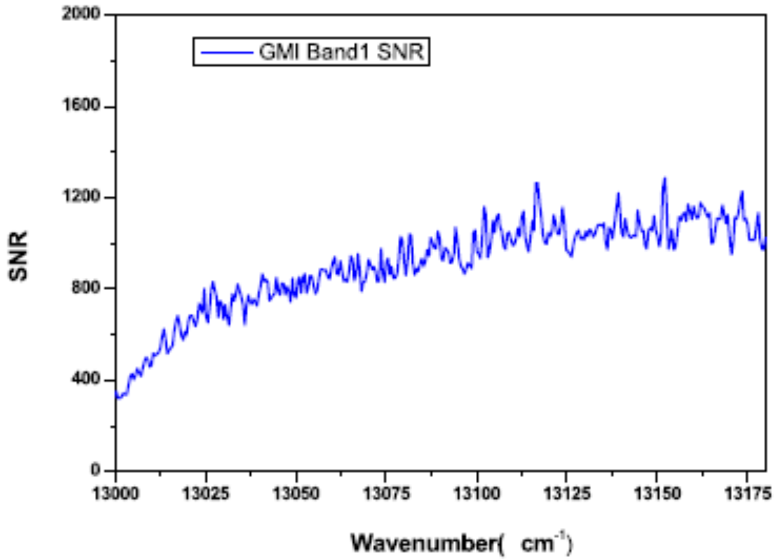

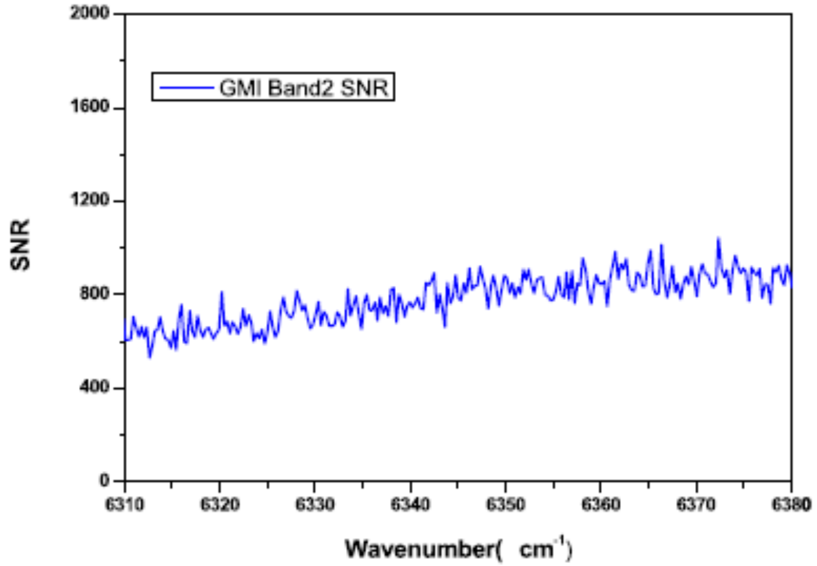

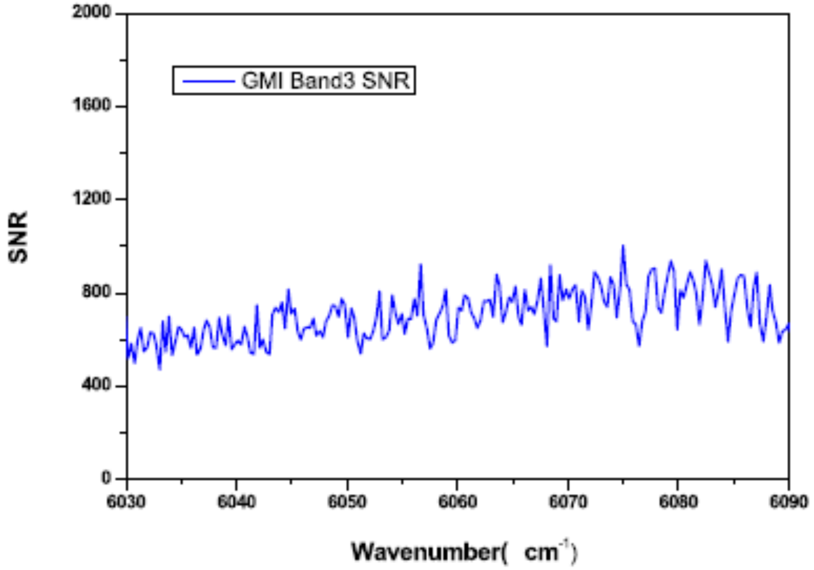

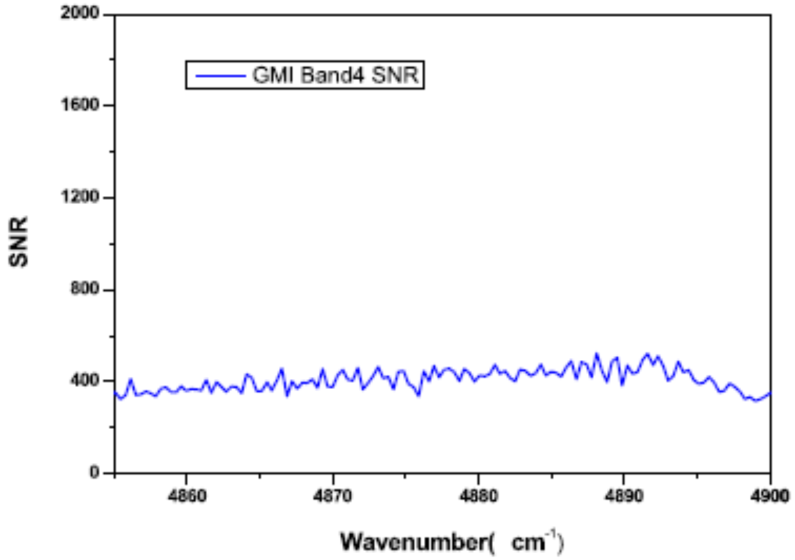

Level 1 Product Results

Spectral Stability

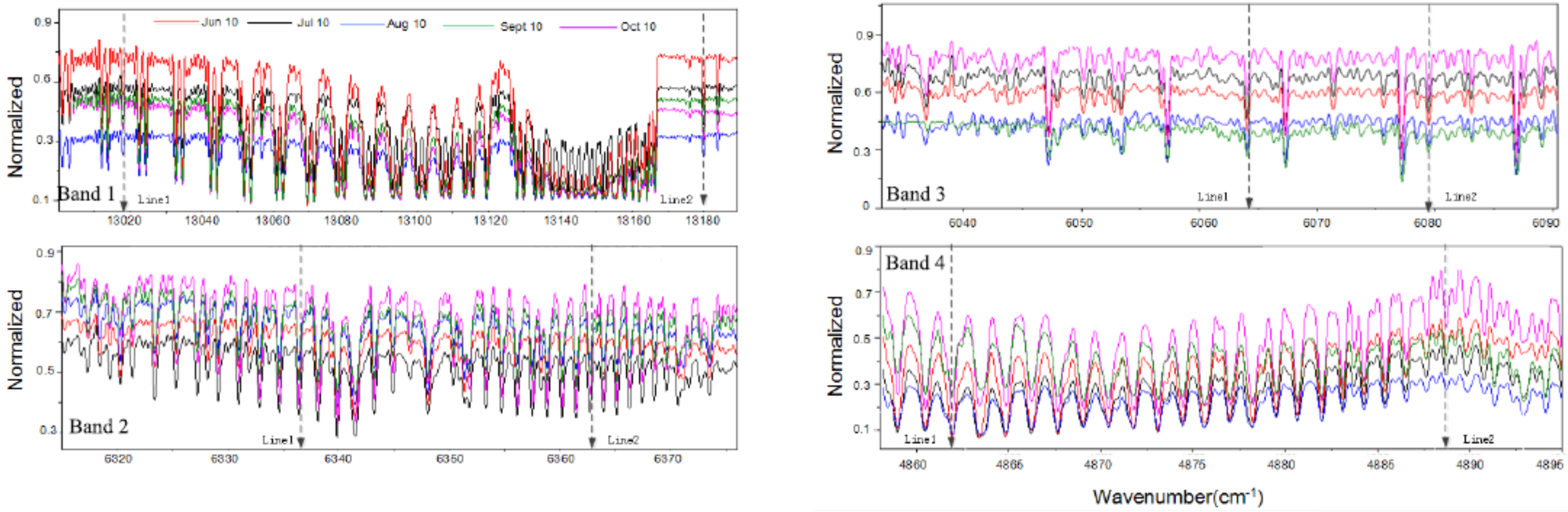

Time (2018)	Band 1 (cm^{-1})		Band 2 (cm^{-1})		Band 3 (cm^{-1})		Band 4 (cm^{-1})	
	Line 1	Line 2	Line 1	Line 2	Line 1	Line 2	Line 1	Line 2
Jun 10	13017.9790	13179.9970	6336.4353	6334.6466	6064.0515	6079.4725	4861.9178	4887.6720
Jul 10	13017.9900	13180.0270	6336.4363	6334.6536	6064.0415	6079.4736	4861.9245	4887.6520
Aug 10	13017.9900	13179.9970	6336.4363	6334.6536	6064.0515	6079.4746	4861.9245	4887.6520
Sept 10	13017.9900	13180.0270	6336.4473	6334.6436	6064.0445	6079.4857	4861.9245	4887.6554
Oct 10	13017.9900	13179.9970	6336.4363	6334.6536	6064.0515	6079.4857	4861.9111	4887.6654
Maximum deviation	0.0200	0.0300	0.0110	0.0102	0.0070	0.0130	0.0130	0.0200

Level 1 Product Results

L1 Product

The independent absorption lines are consistent, and the difference in radiation brightness is small. However, the spectral resolution of the two instruments is not the same, so there is a certain difference in the depth of the absorption peak

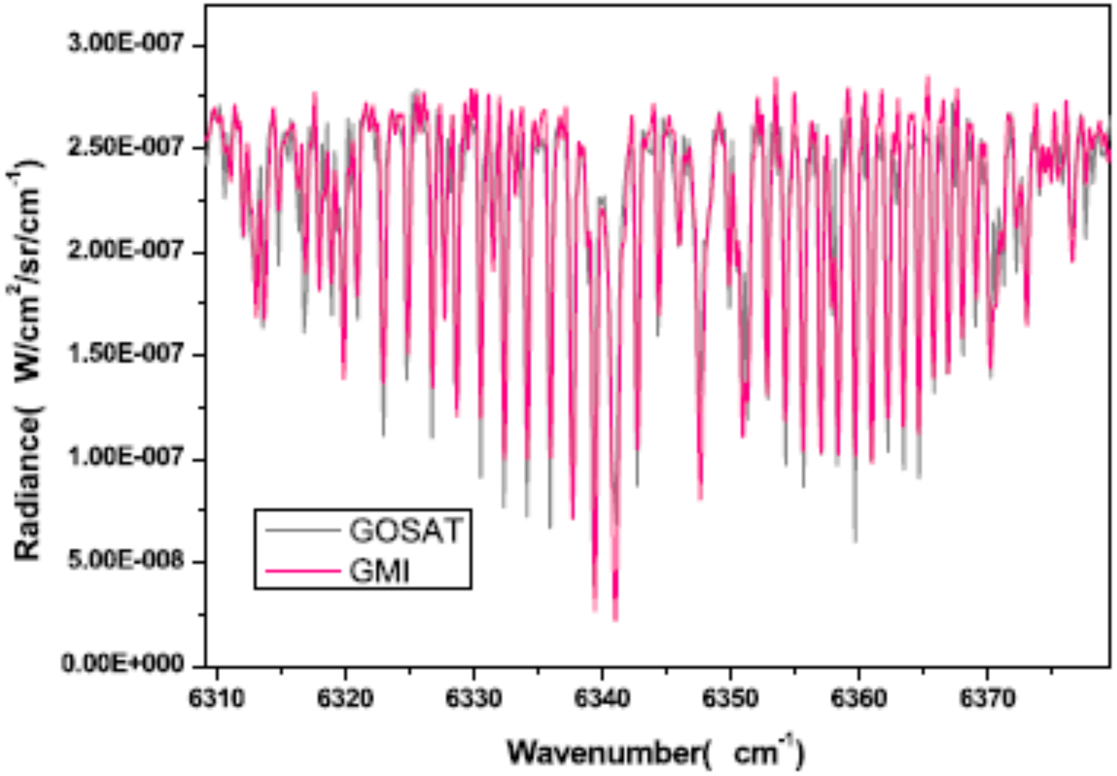

Retrieval Results

$$x_{i+1} = x_a + \left(K_i^{T} S_{\varepsilon}^{-1} K_i + S_a^{-1}\right)^{-1} K_i^{T} S_{\varepsilon}^{-1} \times \left[y - F(x_i) - K_i(x_i - x_a)\right]$$

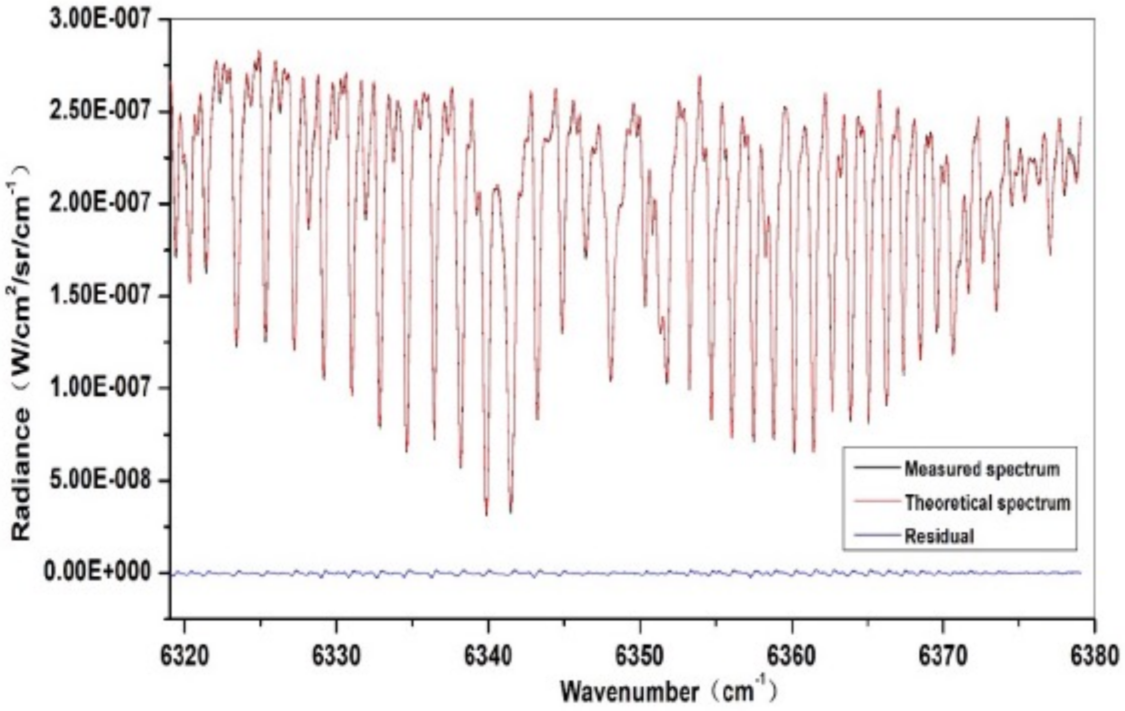

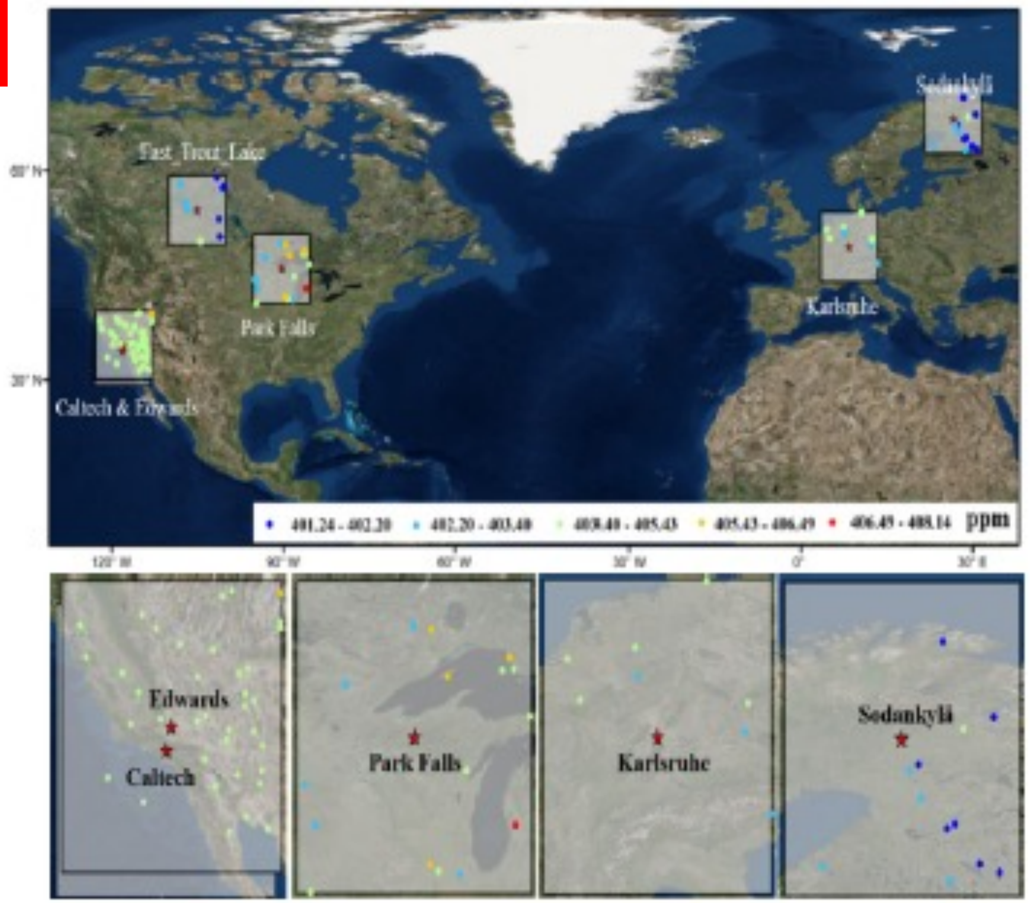

TCCON verification stations and GMI observation points.

Retrieval Results

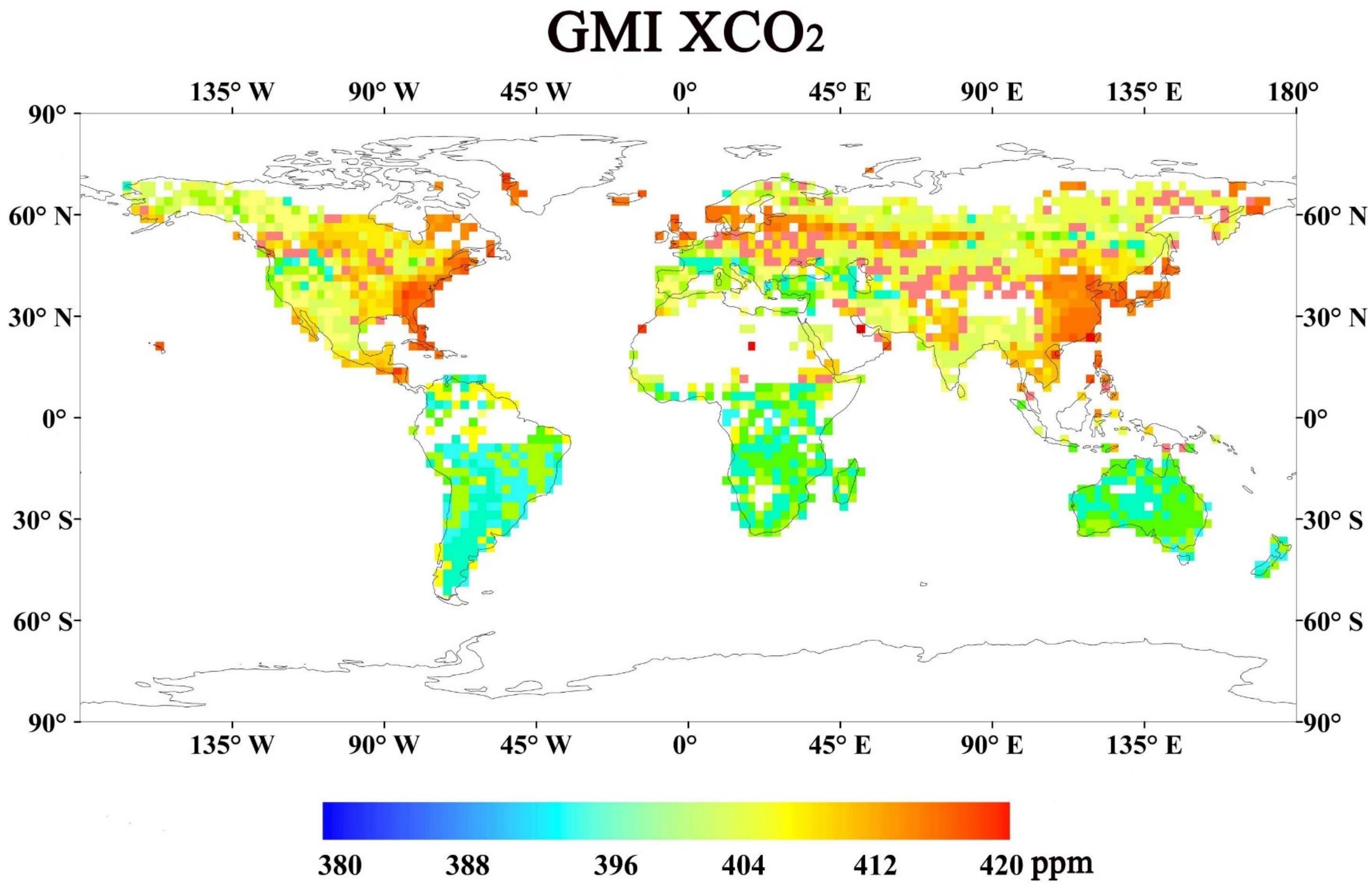

The GMI global atmospheric CO2 measurement results in spring basically cover the land area within the latitude of 70 °, and have a good manifestation of the difference of CO2 concentration between the northern and southern hemispheres. Due to the influence of vegetation in the northern hemisphere in summer, the CO2 concentration in the northern hemisphere is often higher than that in the southern hemisphere.

中国科学院合肥物质科学研究院
Hefei Institutes of Physical Science, Chinese Academy of Sciences

Retrieval Results

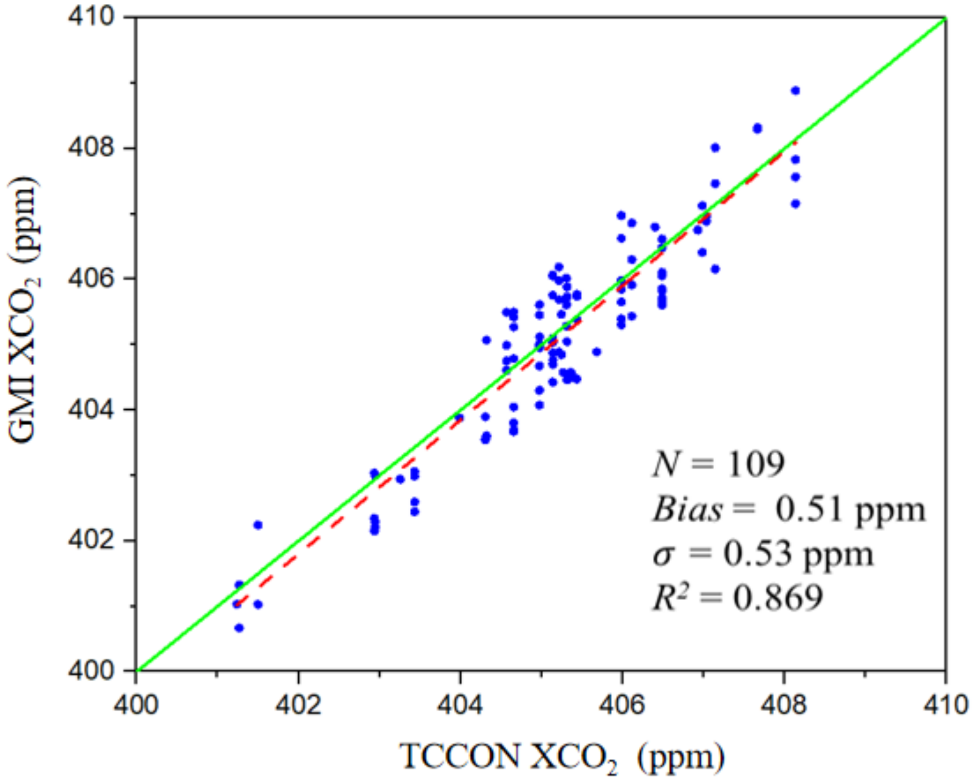

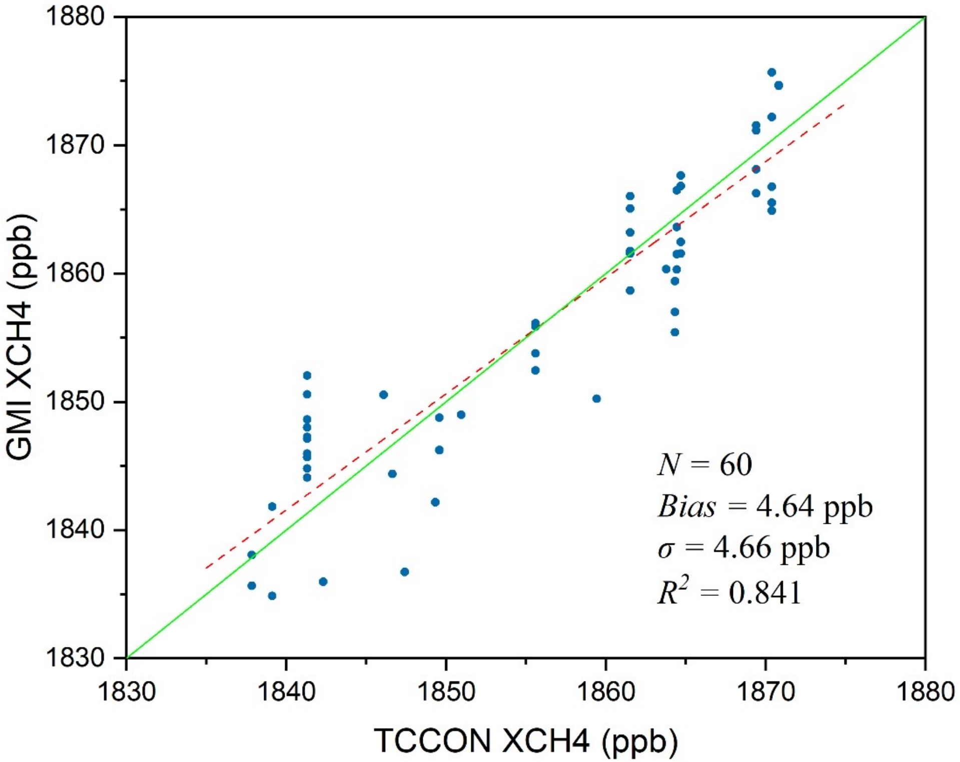

- Enhance the collaborative application of greenhouse gas monitor load GMI and aerosol detector load DPC data on Gaofen 5 satellite;
- Explore the flux calculation of greenhouse gas load GMI and the analysis of global carbon sources and sinks

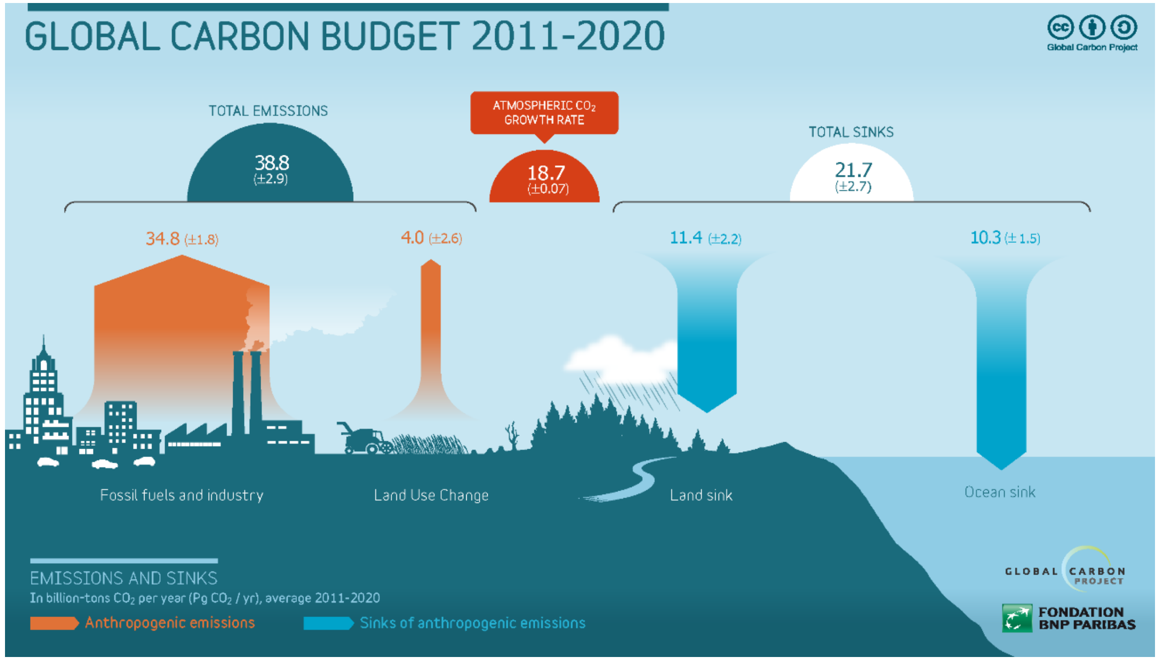

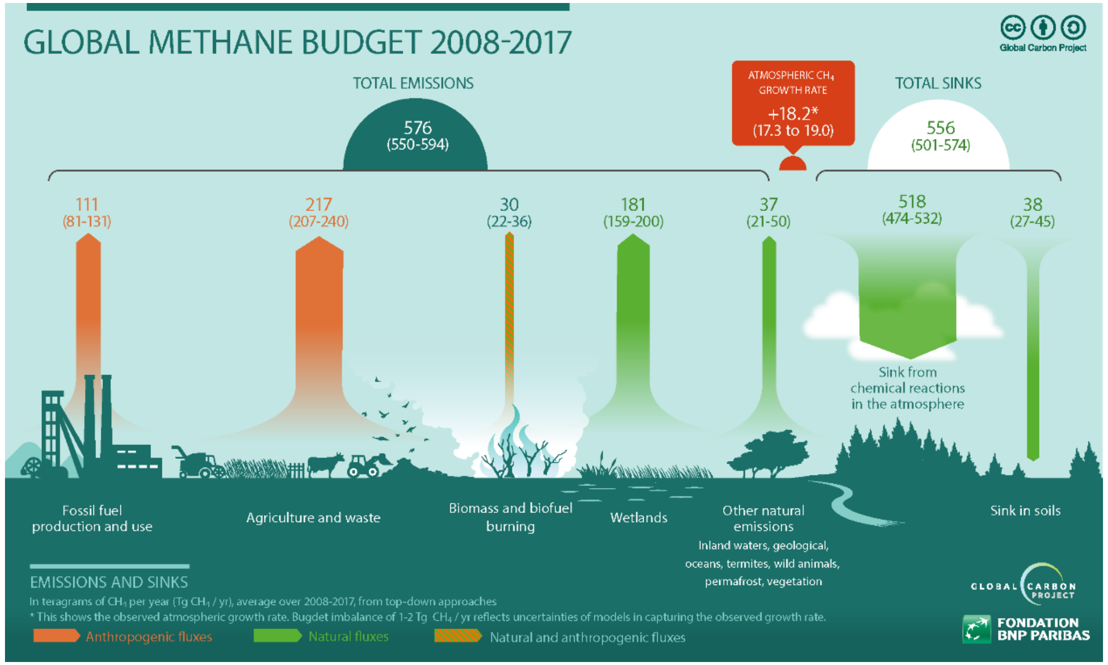

Data source: Friedlingstein et al. 2021 Global Carbon Budget 2021. Earth System Science Data.

Thank you!